STOPPING AND BENDING LIGHT IN 2D PHOTONIC STRUCTURES

Alejandro B. Aceves and Tomáš Dohnal
Department of Mathematics, University of New Mexico, Albuquerque, NM 87131, USA
aceves@math.unm.edu, dohnal@math.unm.edu

Abstract The problem of light propagating through two dimensional photonic structures with a localized defect is addressed. Examples of potential engineering applications of such structures are rerouting of light pulses or optical memory. The governing mathematical model is the system of Coupled Mode Equations (CME) in two spatial dimensions with addition of potentials which account for the defect. As we briefly explain, unlike the one dimensional model of CME without potentials, the two dimensional (x-uniform grating) one does NOT support stable localized pulses as solutions. Because stable pulses are necessary for any physical application, we add grating also in the x direction making, in effect, a true 2D photonic structure, and as we show numerically, this allows for launching of stable pulses. Next, making sensitive assumptions on the shape of the defect, we first give here a derivation of exact linear defect modes, i.e. solutions to the linear system with potentials, and then outline our future study of whether these linear modes persist into the nonlinear regime. Our next future task is to study the interactions of pulses with the nonlinear defect modes.

Keywords: Coupled Mode Equations, planar waveguide, grating, photonic structure, defect mode, stopping light

1. Uniform Grating Structures

1.1 1D Structures - Fiber Gratings

Perhaps the most utilized one dimensional photonic structure is the fiber grating. Here the envelope of the confined transverse (x, y) mode propagates in a medium having a periodic (in z) refractive index profile. Furthermore, the periodicity of the refractive index in the direction of propagation is assumed to be in Bragg resonance with the wavelength of the electric field, thus creating strong back reflection.

The regime of wave propagation through these gratings that we are interested in is when the coupling between forward and backward propagating modes is of the order of the nonlinear length. A coupled system for the slowly varying envelopes of the electric field can be derived from Maxwell's Equations. The derivation is typically done using a multiple scales expansion under the assumption that the characteristic length scales of the coupling and the nonlinearity are in balance. The dynamics in uniform fiber gratings are then governed by the one dimensional Coupled Mode Equations (see for example chapter 2 of [8])

$$\begin{aligned} i(\partial_t + c_g\partial_z)E_+ + \kappa E_- + \Gamma(|E_+|^2 + 2|E_-|^2)E_+ = 0 \\ i(\partial_t - c_g\partial_z)E_- + \kappa E_+ + \Gamma(|E_-|^2 + 2|E_+|^2)E_- = 0, \end{aligned} \tag{1}$$

where E_+, E_- denote the forward and backward propagating envelopes respectively; and without any loss of generality $c_g, \kappa, \Gamma > 0$.

This system has been studied extensively. Although it is not integrable, Chen and Mills showed in [4] that it supports stable solitary wave solutions with frequency inside the forbidden gap of the linear system ($\Gamma = 0$). These are usually called "**gap solitons**" and in theory they can propagate with velocities ranging between 0 and the speed of light in the corresponding uniform medium. A more general class of solitary wave solutions was presented in [3]. The stability of the solitary waves is not all that surprising because in the more realistic experimental scenario (with frequency close to but outside the gap) (1) can be approximated by the Nonlinear Schrödinger Equation (again chapter 2 of [8]).

Gap solitons were later also demonstrated experimentally, see [5]; but the lowest velocity that has been seen experimentally is about $0.5\frac{c}{n}$. The main difference between the gap solitons and true solitons propagating in bare fibers from the applications point of view is the distance at which solutions converge to these stable pulses. The grating allows for a solution to converge to a stable pulse within centimeters whereas in a bare fiber it happens only after hundreds of meters! This is very important for using periodic structures as optical logic and storing devices.

1.2 2D Structures - Planar Waveguide Gratings

A natural extension to the fiber grating is to go to a waveguide geometry, where the confinement of light is only in one (y) transverse direction. In addition to all the features of waves propagating in fiber gratings we get diffraction in the x direction for the planar waveguide gratings. The first question to ask is if by balancing coupling between modes, nonlinearity and diffraction, gap solitons exist.

The two dimensional Coupled Mode Equations

$$\begin{aligned} i(\partial_t + c_g\partial_z)E_+ + \kappa E_- + \partial_{x^2}^2 E_+ + \Gamma(|E_+|^2 + 2|E_-|^2)E_+ = 0 \\ i(\partial_t - c_g\partial_z)E_- + \kappa E_+ + \partial_{x^2}^2 E_- + \Gamma(|E_-|^2 + 2|E_+|^2)E_- = 0 \end{aligned} \tag{2}$$

are derived using the assumption that the characteristic length-scale of diffraction is in balance with the length scales listed for (1).

Just like (1), (2) is dispersive, conservative, not integrable and Hamiltonian. It does not, however, support any stable localized pulses as its solutions. In [2] it is shown that for frequencies close to but outside the linear regime gap the system is well approximated by the 2D NLSE. As a consequence, for sufficiently high powers these solutions have a tendency to collapse (point blowup) but a collapse implies broadening of the solution in the Fourier space and eventual overlap of the spectrum with the frequency gap where the NLSE approximation is no longer valid. Therefore, while localized dynamics in the 2D CME does not lead to collapse, it remains unstable and in particular there are no stationary wave solutions. This can be argued more directly using the Hamiltonian structure. The Hamiltonian functional is

$$\begin{aligned} H = \; & \int_{\mathbb{R}}\int_{\mathbb{R}} ic_g\left(E_+^*\partial_z E_+ - E_-^*\partial_z E_-\right) + \kappa\left(E_-E_+^* + E_-^*E_+\right) - \\ & |\partial_x E_+|^2 - |\partial_x E_-|^2 + \Gamma\left(\tfrac{1}{2}|E_+|^4 + 2|E_-|^2|E_+|^2 + \tfrac{1}{2}|E_-|^4\right)dxdz. \end{aligned}$$

A stationary wave solution would have to be a minimizer of H under the constraint that the total energy (which is conserved) stays constant; $\int\int |E_+|^2 + |E_-|^2 dxdz = \text{const}$. But given a candidate E_+, E_- for the minimizer, we can always perturb it in such a way that we add more x oscillations to increase the negative contribution from the $|\partial_x E_\pm|^2$ terms without changing the L_2 norm of E_+ or E_-. Hence, no minimizer exists. This is an important difference from the 1D case. The nonexistence of stable pulse propagation was seen both in the reduced variational analysis of [1] and in our numerical experiments, where all so far studied localized pulses rapidly diffract in the x direction. How to overcome this is discussed in the next section.

2. Photonic Structures

Because we wish to study capturing and rerouting of light pulses by defects in 2D periodic structures, we also need the pulses to propagate (in a stable fashion) through the uniform periodic medium before they get to the defects. As mentioned in the previous section, periodic structures uniform in x do not allow for such dynamics. That is why we have decided to consider a structure with grating in the x direction as well. This is certainly possible technologically with today's

developments in photonic structures. The governing model is obtained from (2) by addition of a positive $x-$periodic potential. Here we choose $P(x) = \delta(1 + \cos(\nu x))$:

$$\begin{aligned} i(\partial_t + c_g\partial_z)E_+ + \kappa E_- + \partial_{x^2}^2 E_+ + P(x)E_+ + \Gamma(|E_+|^2 + 2|E_-|^2)E_+ = 0 \\ i(\partial_t - c_g\partial_z)E_- + \kappa E_+ + \partial_{x^2}^2 E_- + P(x)E_- + \Gamma(|E_-|^2 + 2|E_+|^2)E_- = 0. \end{aligned} \tag{3}$$

To demonstrate existence of localized pulses, we have performed numerical experiments. In our numerics we use the discontinuous Galerkin scheme with a triangular mesh. Here we choose order 6 in space and an additive Runge-Kutta time integrator of order 4. Fig. 1 shows the plot of $|E_+|, |E_-|$ at $t = 1$ for the case $\delta = 10, \nu = 2$ and with the $z-$shape of the initial condition being a sech function and the $x-$shape determined as the solution of the linear eigenvalue problem

$$G'' + (\lambda + \delta(1 + \cos(\nu x))G = 0 \tag{4}$$

corresponding to the eigenvalue $\lambda \approx -15.7951$. This eigenfunction is well localized on the interval $[-\pi, \pi]$. The above eigenvalue problem is the $x-$part of the linear case in (3). Note that the initial pulses $E_+(t = 0) = E_-(t = 0)$ were centered at the origin.

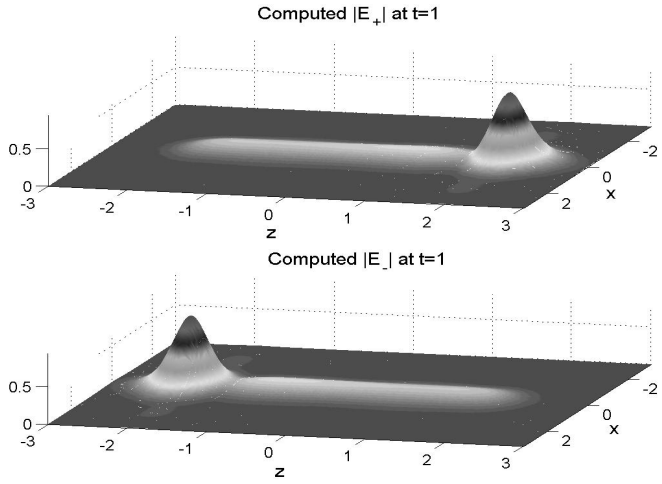

Figure 1. Solution to (3) with $c_g = 2, \kappa = 1, \Gamma = 1$

Although no theory is available for finding exact solutions of (3), one can expect some interplay between gap solitons (for the $z-$dependence) and localized Bloch-type waves, which exist for the time independent NLS with a periodic potential (see [7]).

3. Periodic Structures with Defects

The previous sections dealt with uniform periodic structures which accounted for distinct dynamics. An ongoing research trend is the addition of defects to this structure; an example in linear optics is, by inclusion of a one dimensional defect in a 2D or 3D photonic structure, to bend light beams without radiation loss. For a 1D photonic structure like the fiber grating, by a defect we mean a local variation of the $z-$periodic refractive index. Introducing a defect to a fiber grating allows both for convergence to a stable pulse within centimeters and for manipulating the speed or direction of the pulse propagation due to the effective potential well given by the defect. An appropriate balance between spectral properties of the defect, the velocity and the amplitude of the pulse even allows for a complete stopping of the pulse due to the transfer of its energy into a defect mode. This has potential applications for optical memory or optical switches.

A defect in a planar waveguide grating gives even more potential applications. One can imagine rerouting of pulses into various directions according to their amplitude, using these structures in fiber communications to bend light or, once again, for optical memory.

Goodman, Slusher and Weinstein studied fiber gratings with defects in [6] and showed that capturing of gap solitons is possible. The model, they used, is

$$\begin{aligned} &i(\partial_t + c_g\partial_z)E_+ + \kappa(z)E_- + V(z)E_+ + \Gamma(|E_+|^2 + 2|E_-|^2)E_+ = 0 \\ &i(\partial_t - c_g\partial_z)E_- + \kappa(z)E_+ + V(z)E_- + \Gamma(|E_-|^2 + 2|E_+|^2)E_- = 0. \end{aligned} \tag{5}$$

The authors first studied the linear case, $\Gamma = 0$, and introduced a multiparameter family of defects that support linear bound states (linear defect modes). Their frequency is always in the corresponding frequency gap. Then, by using a perturbative construction, they showed that these defect modes extend into the nonlinear regime. In order to study also large values of the perturbation parameter they did a series of numerical experiments. In these, they managed to verify the principle that a gap soliton interacts most strongly with a defect for which a nonlinear defect mode exists with the same frequency (resonance) and with equal or less total intensity (energetic accessibility).

In our work we wish to apply similar methods for the 2D case. Our first results now follow.

3.1 Linear Defect Modes for the 2D CME

The model we use for the linear regime in two spatial dimensions (without grating in the $x-$direction) is

$$\begin{aligned} i(\partial_t + c_g\partial_z)E_+ + \kappa(z)E_- + \partial_{x^2}^2 E_+ + (V_1(x) + V_2(z))E_+ = 0 \\ i(\partial_t - c_g\partial_z)E_- + \kappa(z)E_+ + \partial_{x^2}^2 E_- + (V_1(x) + V_2(z))E_- = 0. \end{aligned} \tag{6}$$

Note that even if V_1, V_2 have localized effective support (e.g. sech type functions), $V_1(x) + V_2(z)$ does not model a defect strictly localized in a 2D waveguide. Rather it looks like a cross with each line extending over the whole domain. From an application point of view, this should not be a problem because in a real waveguide (or in numerical simulations) this cross can be truncated at some distance from its center (see Fig. 2). Then our analysis on (6) will apply only on the area spanned by the

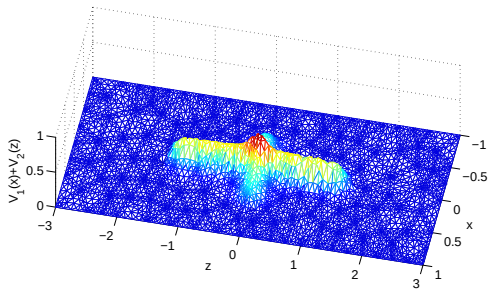

Figure 2. Potential structure used in (6)

cross. We use the potentials V_1, V_2 as given in (6) rather than a more general $V(x,z)$ for simplicity - so that we are able to use separation of variables in (6). Our setup

$$E_\pm = G_\pm(x)F_\pm(z,t) \qquad \text{and} \quad G_+ = G_- =: G$$

gives

$$\left[i\partial_t + ic_g\sigma_3\partial_z + V_2(z) - \mu + \kappa(z)\sigma_1\right]\vec{F} = 0 \tag{7a}$$

$$G'' + (V_1(x) + \mu)G = 0, \tag{7b}$$

with $\sigma_1 = \begin{pmatrix} 0 & 1 \\ 1 & 0 \end{pmatrix}, \sigma_3 = \begin{pmatrix} 1 & 0 \\ 0 & -1 \end{pmatrix}, \vec{F} = \begin{pmatrix} F_+ \\ F_- \end{pmatrix}$ and μ the separation constant.

If, for the $x-$potential, we set, for example, $V_1(x) = 2\beta^2 \mathrm{sech}^2(\beta x)$, the solution to the eigenvalue problem (7b) has a localized eigenfunction. It is $(G, \mu) = \big(\mathrm{sech}(\beta x), -\beta^2\big)$.

With μ fixed, we now try to solve the equation for $\vec{F}$. This can be complicated or impossible for arbitrary grating $\kappa(z)$ and potential $V_2(z)$ but following the ideas in [6] we can obtain exact solutions for some special cases. If we start in the opposite direction, having a form of the solution $\vec{F}$, the problem is easier. For example, setting

$$\vec{F} = e^{-i\omega t} e^{\frac{i}{c_g}\sigma_3 \int_0^z V_2(\xi)d\xi} \vec{L}(z) \qquad \text{with} \quad \omega \in \mathbb{R}, \quad \vec{L}(z) \in \mathbb{R}^2,$$

the problem reduces to a self-adjoint eigenvalue problem for $(\omega, \vec{L})$:

$$\vec{L}' = \begin{bmatrix} i(\omega-\mu) & u(z) \\ \bar{u}(z) & -i(\omega-\mu) \end{bmatrix} \vec{L} \quad \text{with} \quad u(z) = i\kappa(z) e^{\frac{-2i}{c_g}\int_0^z V_2(\xi)d\xi}. \quad (8)$$

The point spectrum is contained in the frequency gap of the linear regime, i.e. $(\mu - |\kappa_\infty|, \mu + |\kappa_\infty|)$, where $\kappa_\infty = \lim_{|z|\to\infty} \kappa(z)$. Setting $u(z) = -e^{i\phi}\left((\omega-\mu) - ik\tanh\left(\frac{k}{c_g}z\right)\right)$ in (8), there is a simple solution

$$\left(\omega - \mu, \begin{pmatrix} 1 \\ ie^{-i\phi} \end{pmatrix} \mathrm{sech}\left(\frac{k}{c_g}z\right)\right).$$

The corresponding grating and potential are easily found

$$\kappa(z) = e^{i\alpha}\left[(\omega-\mu)^2 + k^2 \tanh^2\left(\frac{k}{c_g}z\right)\right]^{1/2}, \quad \alpha \in \{0, \pi\}$$

$$V_2(z) = \frac{1}{2}\frac{k^2(\omega-\mu)\mathrm{sech}^2\left(\frac{k}{c_g}z\right)}{(\omega-\mu)^2 + k^2\tanh^2\left(\frac{k}{c_g}z\right)}.$$

The condition for α is to preserve self-adjointness.

Finally, we can express the whole solution $\begin{pmatrix} E_+ \\ E_- \end{pmatrix}$:

$$e^{-i\omega t}\begin{pmatrix} \exp\left(\frac{i}{2}\arctan\left(\frac{k\tanh\left(\frac{k}{c_g}z\right)}{\omega-\mu}\right)\right) \\ ie^{-i\phi}\exp\left(\frac{-i}{2}\arctan\left(\frac{k\tanh\left(\frac{k}{c_g}z\right)}{\omega-\mu}\right)\right) \end{pmatrix} \mathrm{sech}\left(\frac{k}{c_g}z\right)\mathrm{sech}(\beta x),$$

where $\mu = -\beta^2, \phi - \alpha = \frac{3}{2}\pi$.

Fig.3 shows $|E_+|$ of a numerical solution to (6) with $\kappa(z), V_2(z), V_1(x)$ as given above and the initial condition determined by the above exact solution. The parameters used are $\beta = 7, \omega = -40, k = 4, \phi = \frac{3}{2}\pi$ and $c_g = 1$. The solution is stationary with time invariant modulus.

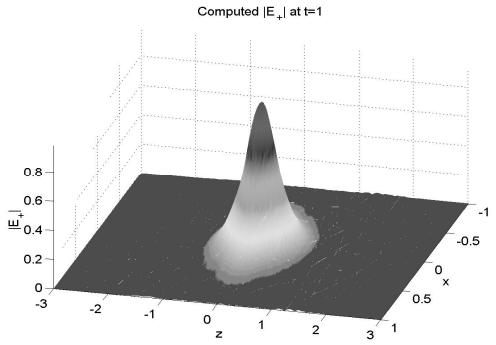

Figure 3. The modulus of a linear defect mode at time $t = 1$

4. Future Work

The linear defect modes, an example of which was given in section 3.1, were not derived for 2D photonic structures, which we have to use in order to achieve stable pulse propagation. Consequently, we will have to change these defect modes to account for the $x-$grating $P(x)$. For each linear frequency ω we will then perform a perturbative construction of a nonlinear defect mode of small total intensity. To continue the bifurcation branch of the mode (and its frequency) for large intensity, we will numerically solve the nonlinear eigenvalue problem

$$\begin{aligned}(\omega + ic_g\partial_z)E_+ + \kappa(z)E_- + \partial_{x^2}^2 E_+ + (V_1(x) + V_2(z) + P(x))E_+ \\ +\Gamma(|E_+|^2 + 2|E_-|^2)E_+ = 0 \\ (\omega - ic_g\partial_z)E_- + \kappa(z)E_+ + \partial_{x^2}^2 E_- + (V_1(x) + V_2(z) + P(x))E_- \\ +\Gamma(|E_-|^2 + 2|E_+|^2)E_- = 0.\end{aligned} \tag{9}$$

It is important to know the temporal frequencies of both the pulse and the defect mode to achieve resonance. Although in the nonlinear case we will probably have to measure the frequency numerically, in the linear case it is easily found from studying the leading exponential tail of each envelope in (3). Taking G the eigenfunction of (4) and substituting

$$\begin{pmatrix} E_+ \\ E_- \end{pmatrix} = \begin{pmatrix} a \\ b \end{pmatrix} G(x)e^{-\vartheta y}e^{-i\omega t}, \quad \text{where} \quad y = z - pc_g t, \Re(\vartheta) > 0, p \in [0,1]$$

into the linear case of (3), we obtain $\omega = \lambda - ic_g\vartheta p \pm \sqrt{\kappa^2 - c_g^2\vartheta^2}$.

Next, we realize that although we have numerically shown that photonic structures (grating in both z and x directions - see section 2) allow

for propagation of localized pulses, in our results, initial data break into two localized states travelling at high speeds, with the forward (backward) bullet having a predominant E_+ (E_-) component. Referring to the 1D case where for the gap solitons E_+, E_- both co-exist moving in one direction, we wish to determine whether a specific $z-$profile in the initial condition allows for such propagation in our 2D case.

Finally, we will investigate the possibility of trapping these pulses on defects as well as changing direction of their propagation due to the contact with a defect. We expect the same principles of resonance and energetic accessibility to hold as in [6] .

Acknowledgments

The research of A.B. Aceves and T. Dohnal is supported by the Army Research Office Grant DAAD19-03-1-0209. The authors thank Timothy Warburton and Thomas Hagstrom (both University of New Mexico) for assistance with the numerical parts of the research.

References

[1] A.B.Aceves, B.Constantini and C.De Angelis, "Two-dimensional gap solitons in a nonlinear periodic slab waveguide," Journ. of the Opt. Soc. Am B **12**, 1475 (1995).

[2] A.B.Aceves, G.Fibich and B.Ilan, "Gap Solitons in Waveguide Gratings," (to appear in Physica D).

[3] A.B.Aceves and S.Wabnitz, "Self induced transparency solitons in nonlinear refractive media," Physics Letters A **141**, 37 (1989).

[4] W.Chen and D.L.Mills, "Gap solitons and the nonlinear optical response of superlattices," Phys. Rev. Lett. **58**, 160 (1987).

[5] B.J.Eggleton, R.E.Slusher, C.M.de Sterke, P.A.Krug and J.E.Sipe, "Bragg grating solitons," Phys. Rev. Lett. **76**, 1627 (1996).

[6] R.H.Goodman, R.E.Slusher and M.I.Weinstein, "Stopping light on a defect," Journ. of the Opt. Soc. Am B **19**, 1635 (2002).

[7] P.J.Y. Louis, E.A. Ostrovskaya, C.M. Savage and Yu.S. Kivshar, "Bose-Einstein condensates in optical lattices: Band-gap structure and solitons," Phys. Rev. A **67**, 013602 (2003).

[8] R.E.Slusher, B.J.Eggleton, "Nonlinear Photonic Crystals," Springer-Verlag, New York, 2003.